Metallophysics and Advanced Technologies
Металофіз. новітні технол.
Metallofiz. Noveishie Tekhnol.
2024, vol. 46, No. 3, pp. 199–210
https://doi.org/10.15407/mfint.46.03.0199
Reprints available directly from the publisher

PACS numbers: 61.50.Lt, 71.15.Ap, 71.15.Mb, 71.15.Nc, 71.20.Nr, 71.27.+a, 81.05.Zx

Electronic Structure of Aluminium Nitride and Its Solid Solutions with Oxygen and Aluminium

V. M. Uvarov, E. M. Rudenko, Yu. V. Kudryavtsev, M. V. Uvarov, I. V. Korotash, and M. V. Dyakin

G. V. Kurdyumov Institute for Metal Physics, N.A.S. of Ukraine,
36 Academician Vernadsky Blvd.,
UA-03142 Kyiv, Ukraine

Using band-structure calculations within the FLAPW (Full-Potential Linearized Augmented-Plane-Wave) model, information is obtained regarding the energy, charge and spatial characteristics of aluminium nitride and its solid solutions with oxygen and aluminium. As established, the formation of these solutions is accompanied by a reduction in electron density in their interatomic regions. The accompanying decrease in the covalence of interatomic interactions leads to both a reduction in binding energies and an increase in the volumes of elementary cells within the compounds. The transition from aluminium nitride to its energetically 'nearest' oxide is accompanied by a decrease in binding energy by 1.25 eV, which corresponds to over $14.5 \cdot 10^3$ K on the temperature scale. This correlation underscores the high resistance of aluminium nitride to oxidation processes. The formation of an alloy with aluminium incorporation becomes even less likely due to the larger decrease in binding energy by 2.84 eV.

Key words: band-structure calculations, alloys, band structure, aluminium nitride, solid solutions.

За допомогою зонних розрахунків у моделі FLAPW (the full-potential linearized augmented-plane-wave) одержано інформацію про енергетичні, зарядові та просторові характеристики нітриду Алюмінію та його твердих розчинів — моделів з Оксиґеном та Алюмінієм. Встановлено, що утворення розчинів супроводжується зменшенням густини електронів у мі-

Corresponding author: Viktor Mykolayovych Uvarov
E-mail: uvarov@imp.kiev.ua

Citation: V. M. Uvarov, E. M. Rudenko, Yu. V. Kudryavtsev, M. V. Uvarov, I. V. Korotash, and M. V. Dyakin, Electronic Structure of Aluminium Nitride and Its Solid Solutions with Oxygen and Aluminium, *Metallofiz. Noveishie Tekhnol.*, **46**, No. 3: 199–210 (2024). DOI:10.15407/mfint.46.03.0199

жатомових областях. Супутнє пониження ковалентности міжатомових взаємодій приводить до зменшення енергій зв'язку та збільшення об'єму елементарних комірок сполук. Перехід від нітриду Алюмінію до його енергетично «найближчого» оксиду супроводжується зменшенням енергії зв'язку на 1,25 еВ, що в температурній шкалі становить понад $14{,}5 \cdot 10^3$ К. Це корелює з високою стійкістю нітриду Алюмінію до процесів його окиснення. Формування стопу втілення з Алюмінієм виявляється ще більш малоймовірною подією з причини ще більшого зменшення його енергії зв'язку — на 2,84 еВ.

Ключові слова: зонні розрахунки, електронна будова, нітрид Алюмінію, тверді розчини.

(Received 22 August, 2023; in final version, 22 August, 2023)

1. INTRODUCTION

Aluminium nitride is an insulator with a wide bandgap, and its unique properties have made it highly promising for applications in high technologies. It is an electronic ceramic characterized by high resistivity [1], good dielectric strength [2], high hardness [3], and a coefficient of thermal expansion close to that of silicon [4]. It also exhibits resistance to oxidation and wear, along with outstanding thermal conductivity comparable to highly conducting metals like aluminium [5]. These properties are also preserved in AlN films [6, 7]. Mentioned properties make AlN an ideal candidate for use in microelectronics substrates. AlN high strength, stability, and corrosion resistance allow its utilization in extreme conditions. The melting temperature of AlN is not precisely defined, but there are some indications [8] suggesting it lies approximately within the range close to 3000 K. Due to its piezoelectric properties, aluminium nitride is also employed in thin-film microwave acoustic resonators [9].

The partially mentioned properties and a range of practical applications of aluminium nitride have spurred extensive research into methods of its synthesis, as well as its structural, optical (including in the infrared range), and electrical properties [10–16].

At atmospheric pressure and room temperature, AlN crystallizes into a hexagonal wurtzite (WZ) structure with the spatial symmetry group $P63mc$ (No. 186) and four atoms per unit cell [17]. Epitaxially grown AlN on most substrates maintains the stable wurtzite structure, but there are also reports [8, 18] of its zinc blende (ZB) structure. The ZB structure remains stable for film thicknesses not exceeding 1.5–2.0 nm. For greater film thicknesses, ZB transforms into the WZ structure [19]. Under pressure ($\cong$ 14–22 GPa), AlN undergoes a transformation from the WZ structure to a cubic NaCl-type (rock salt—RS) structure [17, 20, 21].

The charge density determined from x-ray diffraction experiments [22] suggests that the chemical interatomic bonds in aluminium nitride (hereafter referred to as its WZ-modification) are highly ionic. However, the acceptance of a tetrahedrally co-ordinated wurtzite structure under ambient conditions rather than that of a rock salt structure indicates the presence of some degree of covalence. This is also consistent with the fracture toughness exhibited by AlN, which might be attributed to its partially covalent nature [13]. Spectroscopic investigations of AlN include techniques such as combination scattering and infrared spectra [14–16, 23], reflection and transmission spectra [24], x-ray emission spectra [25]. Ultraviolet photoemission spectroscopy (UPS), electron energy loss spectroscopy (EELS), and Auger spectra have been reported [26, 27]. Elastic and piezoelectric characteristics, as well as dielectric permittivity, have been calculated based on measured phase velocities of surface acoustic waves [28].

In the optical absorption spectra of AlN films with micron thicknesses, several components have been identified [12], including energies of 4.5 and 4.8 eV, and a peak with maximum intensity at 6.2 eV. A low-energy peak at 2.8 eV has also been reported in a study [29]. Low-energy features in the spectra are often associated with oxygen-related impurities, while the component with maximum intensity at 6.2 eV is attributed to the excitation of valence electrons to the conduction band of AlN [12 and references therein]. This value is currently accepted as the experimentally determined bandgap width of aluminium nitride.

Depending on the quantum mechanical calculation methodologies employed, the direct bandgap energies of aluminium nitride have been obtained with values ranging from 2.35 to 5.31 eV [30–33]. In a study [34], using a semi-empirical tight-binding method, a value of 6.2 eV was obtained for the direct bandgap energy.

Currently, aluminium oxynitride (AlON) is attracting significant attention due to its potential applications as optical windows, transparent armour, dome materials, and LED lighting [35, 36]. One of the simplest methods for producing AlON is the solid-state reaction between aluminium nitride and aluminium oxide, conducted at temperatures above 1700°C for several hours [37].

Promising for the production of high-quality AlN and AlON films is the vacuum helicon-arc ion-plasma technology developed by the authors, which allows to obtain high-quality films of ion-plasma condensates on dielectric and conductive substrates at temperatures of 50–300°C [38–40].

In this context, it becomes interesting to consider a model problem of introducing oxygen atoms directly into the aluminium nitride matrix. The same holds true for the aluminium-saturated compound Al_3N_2, which can be regarded as a model for simulating the processes of aluminium doping in AlN, forming an interface layer at the boundary

of aluminium nitride and an aluminium substrate.

It is worth noting that none of the mentioned studies have employed a unified and comprehensive approach to investigating crucial electronic structure characteristics of the mentioned compounds, such as binding energies, atomic charge states, valence and conduction band structures, and the nature of interatomic chemical bonds. Comparative analyses of the electronic structures of these compounds are of particular interest.

This work is dedicated to addressing mentioned issues.

2. CALCULATION METHODOLOGY

In this study, electronic structure band calculations were conducted for aluminium nitride and its solid solution-models with oxygen and aluminium. The elementary unit cells of the investigated compounds, labelled by the values $K = 1–7$ (K—atomic configuration) and arranged in order of decreasing binding energies (Fig. 2), are presented in Fig. 1. The structure of the $K = 1$ initial aluminium nitride belongs to the hexagonal symmetry with $P63mc$ space group (No. 186) [41]. Interstitial solid solution involving oxygen and aluminium, as depicted in Fig. 1, are represented by elementary unit cells $K = 2$ and $K = 4$. On the other

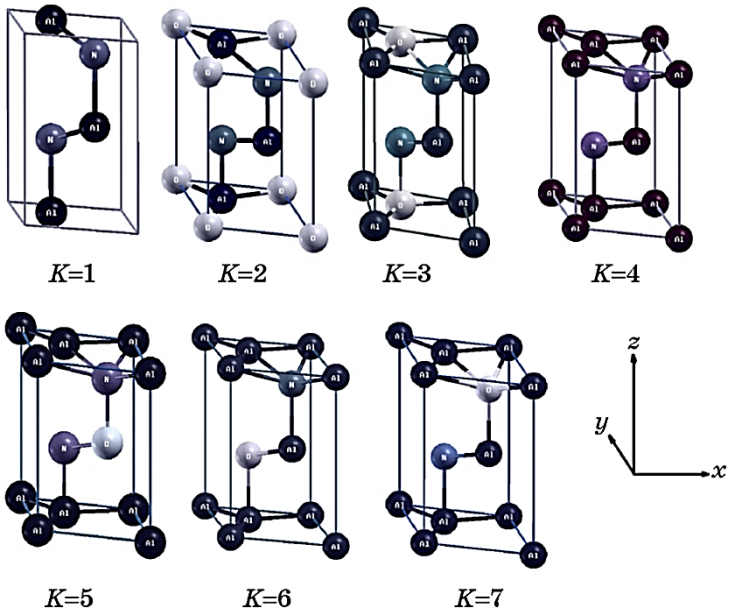

Fig. 1. Elementary cells of aluminium nitride ($K = 1$) and its compounds with oxygen and aluminium. The co-ordinate system is the same for all cells. Here and further in the figures K is the atomic configuration.

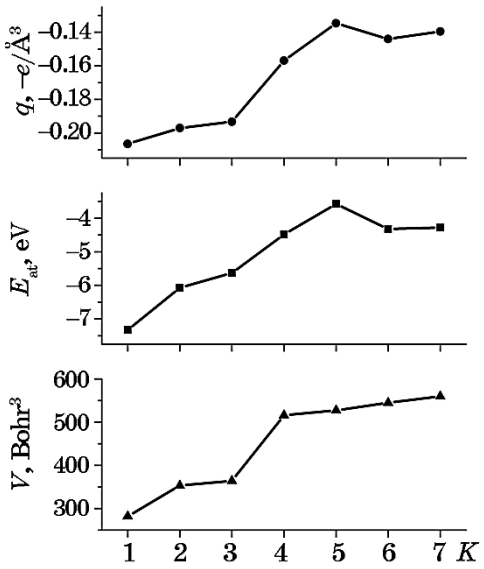

Fig. 2. Spatial electron densities (q, e—electron charge) in interatomic regions, average binding energies per atom (E_{at}) and volumes (V) of elementary cells of compounds.

hand, the remaining cells obtained from Al_3N_2 simulate solutions in which oxygen atoms replace atoms in the structure of the 'body' of AlN itself.

The band calculations were carried out using the LAPW (Linear Augmented Plane Wave) approximation [42] with the generalized gradient approximation (GGA) for electronic density in the form [43]. The scalar-relativistic variant of the LAPW method [44] was employed to calculate the electronic structure characteristics of the compounds. The positions of atom components in the structure of the investigated compounds were determined using symmetry operations of a simple hexagonal lattice H and the information provided in the Table 1. Here, the coordinates of aluminium and nitrogen atoms with indices 1 and 2 represent the structure of AlN. The structures of the remaining alloy models were simulated by sequentially replacing oxygen atoms with atoms in the $K = 4$ cell.

The muffin-tin (MT) radii of atomic spheres were selected to minimize the size of the interstitial region (II) in the $K = 1$ modification, which has the smallest volume of the elementary cell. For all spatial configurations and all atoms, these radii were set at 1.69 Bohr (1 Bohr = $5.2918 \cdot 10^{-11}$ m). In the electronic structure calculations of all compounds, 168 points were used in the irreducible parts of their Brillouin zones. The product of the MT sphere radius (R_{mt}) and the maximum value of the wave vector for plane waves (K_{max}) was chosen to be

TABLE 1. The positions of atoms in the structure of the Al_3N_2 alloy in the fractions of the edges of the unit cell ($K = 4$).

	x	y	z
Al_1	1/3	2/3	0.0
Al_2	2/3	1/3	0.5
N_1	1/3	2/3	0.381
N_2	2/3	1/3	0.881
Al_3	0.0	0.0	0.0

seven, with maximum values of the quantum number l set to 10 for partial waves within spheres and $l = 4$ in calculations of non-muffin-tin matrix elements.

As there is no literature information available on the values of lattice parameters for the hexagonal lattices associated with solid solutions of aluminium nitride, they were calculated using a spatial structure minimization procedure [44].

The binding energies (cohesive energies) were calculated as the differences between the total energies of the compounds themselves and the sums of the total energies of the constituent atoms when they are infinitely separated from each other. The latter were determined according to the recommendations [45].

3. RESULTS AND DISCUSSION

The sequential transition from aluminium nitride with an elementary cell configuration of $K = 1$ to its solid solution with $K = 7$ is accompanied by a decrease in the electron density within the interatomic region of the investigated compounds (Fig. 2). This circumstance indicates [46] the accompanying reduction in the covalence of interatomic interactions, which in turn leads to a decrease in binding energies and an increase in the volumes of the elementary cells of the compounds. From the discussed graph, it's evident that the behaviour of the curves for E_{at} (binding energies) and V (volumes) is essentially governed by and aligns with the charge densities in the interatomic regions of the compounds. The covalent bonds are most loosened in the compounds with $K = 5–7$. As apparent from the values of binding energies (E_{at}) of these compounds, they turn out to be the least stable. Thus, the formation of stable oxides with substituted nitrogen atoms appears to be an improbable process. The transition from aluminium nitride to its energetically 'closest' oxide with $K = 2$ is accompanied by a decrease in binding energy of $\Delta E_{at} = 1.25$ eV, which in terms of temperature corresponds to over $14.5 \cdot 10^3$ K. These facts point to the high resistance of aluminium

nitride to oxidation and corrosion processes. On the other hand, the formation of the insertion alloy Al_3N_2 ($K = 4$) becomes an even more improbable event due to the larger value of $\Delta E_{at} = 2.84$ eV.

The energy band structures $E(\mathbf{k})$ of the investigated compounds are presented in Fig. 3. It is evident that aluminium nitride itself ($K = 1$) and the oxide with substituted nitrogen atom within the AlN structure ($K = 7$) are insulators. The energy bandgap (E_{Gap}) in the aluminium nitride structure is 4.2 eV, and it is a direct bandgap concentrated at the Γ point of the Brillouin zone. The obtained value of E_{Gap} was noticeably lower than the experimentally determined value, reflecting the general trend of underestimated values obtained in band calculations (see introduction). One possible reason for this can be attributed to the fact that most band calculations do not accurately describe excited final states of electrons, which are observed in experiments. A direct energy gap localized in the interval from Λ–Γ in the Brillouin zone is present in the $E(\mathbf{k})$ spectrum of the oxide with $K = 7$, with a value of $E_{Gap1} = 0.25$ eV. A smaller energy gap $E_{Gap2} = 0.23$ eV is indirect, corresponding to electronic transitions involving phonons from $K \rightarrow \Lambda$–Γ. The remaining band structures ($K \neq 1, 7$) in Fig. 3 are typical of compounds characteristic of metals.

The charge states of the atoms within the investigated compounds

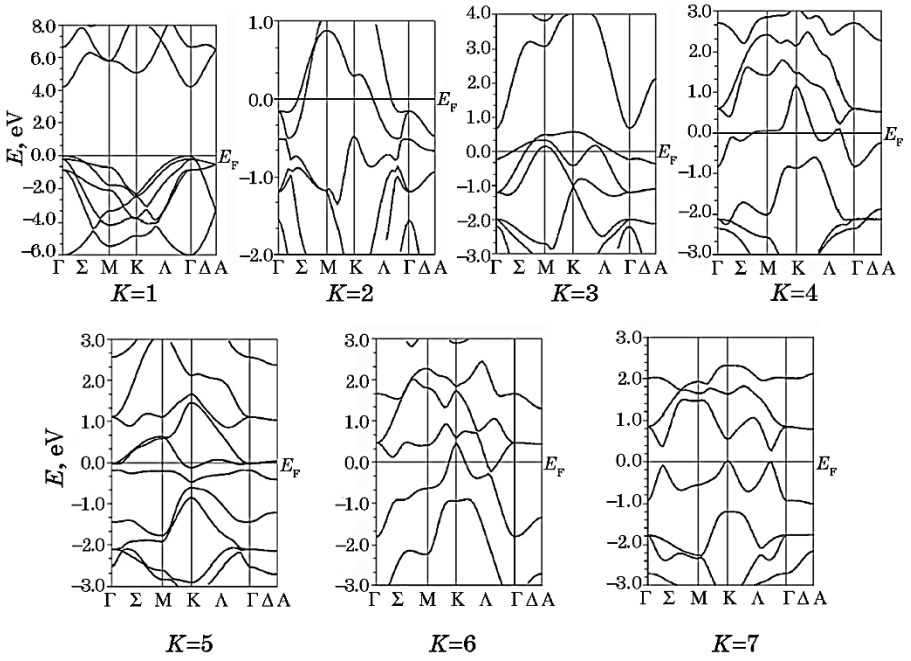

Fig. 3. Energy band structure $E(k)$ of aluminium nitride ($K = 1$) and its solid solutions with aluminium ($K = 4$) and oxygen ($K \neq 1, 4$).

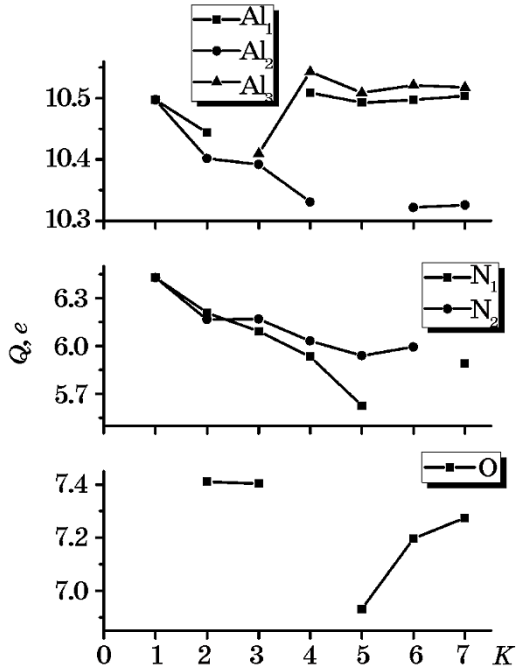

Fig. 4. Atomic charges (Q, e—electron charge) of compounds.

exhibit a compensatory nature, where an increase in charge on certain atoms is accompanied by a decrease on other types of atoms (see Fig. 4). For instance, the reduction in the charges of nitrogen and Al_2 atoms, which are genetically linked to aluminium nitride and form the central region of its elementary cell, is correspondingly associated with an anomalous redistribution of charges onto oxygen atoms in the structures with $K = 2$ and $K = 3$. Further, the almost monotonic decrease in the charges on the mentioned atoms in structures with $K \geq 4$ is accompanied by an increase in the charge states of the remaining aluminium and oxygen atoms. It is noteworthy that, in the $K = 5$ structure with the central oxygen atom, its charge reaches a minimum value of 6.93 units of electron charge.

Figure 5 shows the total and atomic electron densities of some of the investigated compounds. The structure of their valence bands consists of two subzones—one localized near the energy level of –15.0 eV, and the other is concentrated in the interval of –8.0 to 0.0 eV.

The first subzone is predominantly represented by s-states of nitrogen atoms, which are genetically linked to its quasi-core $2s$ electrons. In the solid solution with oxygen incorporation ($K = 2$), the discussed states are hybridized, while in structures with larger values of $K = 4$, 5, they appear as distinct peaks, reflecting their atomization. In the

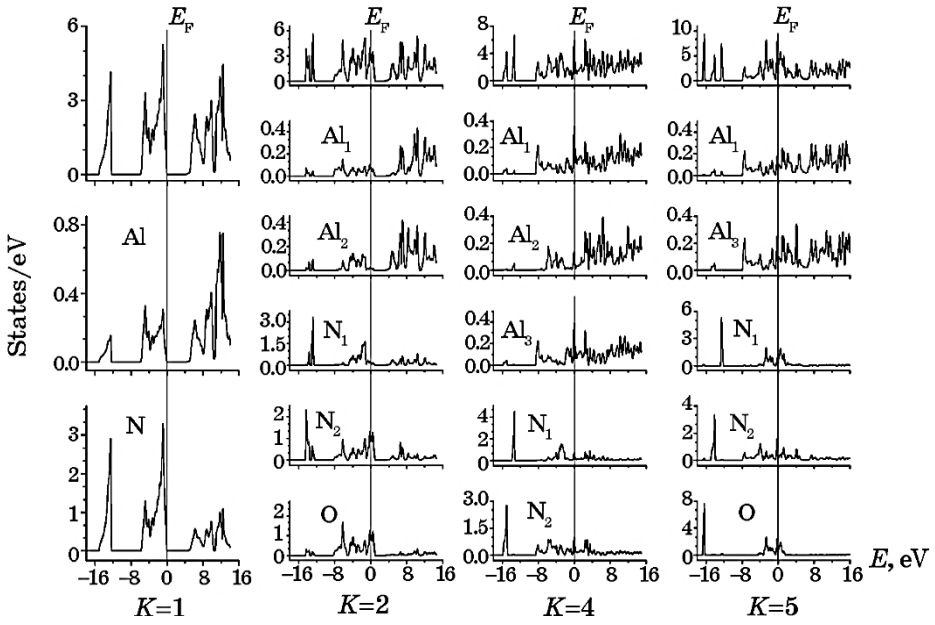

Fig. 5. Full (upper panels in each column of the figure) and full atomic electron densities of compounds. Vertical thin lines indicate the energy positions of the Fermi levels (E_F).

case of the oxide with $K = 5$, states of oxygen atoms with the same symmetry and genetics as well as high degree of atomization also appear in this energy zone. The mentioned atomization and, as a consequence, the reduction in interaction among the discussed atoms due to their quasi-core electrons, are caused by the difference in the charge states of nitrogen and oxygen atoms (see Fig. 4). Indeed, the lower the charge of one of the nitrogen atoms, the lower the binding energy (in absolute terms) of its quasi-core electrons—the corresponding peak in the electron densities will 'emerge' towards the Fermi level and vice versa. It's worth noting that the observed atomization correlates with the decrease in the binding energies of the compounds as their configurations transition to larger K values (see Fig. 2). This emphasizes the importance of considering interactions involving the quasi-core electrons of nitrogen when examining the chemical aspects of compound formation with its participation.

The second subzone is formed by hybridized states of nitrogen and aluminium atoms, and in the case of oxides, states of oxygen atoms are added to the hybridization region. In this hybridization, p-symmetry electrons from all the atoms of the compounds participate, and aluminium's s-electrons, which are primarily localized at the bottom (Al_1, Al_3), the middle (Al_2), and near the Fermi level (Al_3) of the subzone, al-

so contribute to the formation of the band. In turn, the conduction band of the compounds is primarily formed by *s* and *p*-states of nitrogen and aluminium atoms. As evident from the discussed results presented in Fig. 5, in the oxides and solid solution Al_3N_2, there are peaks of high intensity in the electronic density of states directly at the Fermi level. Typically, the presence of such components in the electronic density of states of compounds indicates a reduction in their thermodynamic stability. Upon transitioning from $K = 2 \rightarrow K = 4 \rightarrow K = 5$, the intensity of Fermi level components increases in the sequence of $2.3 \rightarrow 5.8 \rightarrow 7.9$ density units, respectively. The progressive decrease in stability among the discussed compounds is also confirmed by their binding energies (Fig. 2).

4. CONCLUSIONS

1. The formation of solid solutions of aluminium nitride with oxygen and aluminium is accompanied by a decrease in the electron density in their interatomic regions. The simultaneous reduction in the covalence of interatomic interactions leads to a decrease in binding energies and an increase in the volumes of elementary cells in the compounds. The transition from aluminium nitride to its energetically 'nearest' oxide is accompanied by a decrease in binding energy by 1.25 eV, corresponding to over 14.5×10^3 K on the temperature scale. This explains the high resistance of aluminium nitride to oxidation processes. The formation of an alloy with aluminium is even more unlikely due to a larger reduction in its binding energy by 2.84 eV.
2. Most of the compounds modelling the processes of forming solid solutions of aluminium nitride with oxygen and aluminium exhibit metallic behaviour. The charge states of atoms in the investigated compounds have a compensatory nature—an increase in the charge on some atoms is accompanied by a decrease in charge on other types of atoms.
3. The structure of the valence bands of aluminium nitride and its solid solutions consists of two subzones—one of them is localized near the energy level of –15.0 eV, and the second is concentrated in the range of –8.0 to 0.0 eV.
4. The first subzone is predominantly formed by *s*-states of nitrogen atoms, genetically linked to its quasi-core 2*s*-electrons. In the solid solution with oxygen incorporation, the discussed states are hybridized, whereas in the remaining compounds, they are represented by individual peaks reflecting their atomic character. This atomization correlates with the decrease in bond energies of the compounds, indicating the importance of considering the interactions of nitrogen's quasi-core electrons when examining the chemical aspects of compound formation involving nitrogen.
5. The second subzone is formed by hybridized states of nitrogen and

aluminium atoms, while in oxides, states of oxygen atoms are added to the hybridization region. In this hybridization, *p*-symmetry electrons of all atoms in the compounds are involved, and aluminium *s*-electrons contribute to the formation of the band too. The conduction band of the compounds is predominantly shaped by s and *p*-states of nitrogen and aluminium atoms.

6. In the electronic densities of solid solutions of aluminium nitride with oxygen and aluminium, high-intensity components are present at the Fermi level. The intensities of these components correlate with the binding energies of the compounds and can be used as one of the criteria to determine their thermodynamic stability.

The authors are grateful to the National Academy of Sciences of Ukraine for partial support within the framework of the projects 4.2/23-П of the budget program 'Support for the development of priority areas of scientific research' (КПКВК 6541230) and ІМФ-2022/1 (КПКВК 6541230).

REFERENCES

1. A. W. Weimer, G. A. Cochran, G. A. Eisman, J. P. Henley, B. D. Hook, L. K. Mills, T. A. Guiton, A. K. Knudsen, N. R. Nicholas, J. E. Volmering, and W. G. Moore, *J. Am. Ceram. Soc.*, **77**: 3 (1994).
2. A. V. Virkar, T. B. Jackson, and R. A. Cutler, *J. Am. Ceram. Soc.*, **72**: 2031 (1989).
3. T. J. Mroz, Jr., *Am. Ceram. Soc. Bull.*, **71**: 782 (1992).
4. P. T. B. Shaffer and T. J. Mroz, Jr., *Aluminum Nitride* (Advanced Refractory Technology, Inc., 1991).
5. A. Glen, R. A. Slack, R. Tanzilli, O. Pohl, and J. W. Vandersande, *J. Phys. Chem. Solids*, **48**: 141 (1987).
6. O. Ye. Pogorelov, O. V. Filatov, E. M. Rudenko, I. V. Korotash, and M. V. Dyakin, *Progress in Physics of Metals*, **24**, No. 2: 239 (2023).
7. E. M. Rudenko, A. O. Krakovnyy, M. V. Dyakin, I. V. Korotash, D. Yu. Polots'kyy, and M. A. Skoryk, *Metallofiz. Noveishie Tekhnol.*, **44**, No. 8: 989 (2022) (in Ukrainian).
8. A. Siegel, K. Parlinski, and U. D. Wdowik, *Phys. Rev. B*, **74**, 104116 (2006).
9. G. R. Kline and K. M. Lakin, *Appl. Phys. Lett.*, **43**, 750 (1983).
10. H. Vollstadt, E. Ito, M. Akaishi, S. Akimoto, and O. Fukunaga, *Proc. Japan Acad.*, 66, Ser. B: 7 (1990).
11. I. Petrov, E. Mojab, R. C. Powell, J. E. Greene, L. Hultman, and J.-E. Sundgren, *Appl. Phys. Lett.*, **60**: 2491 (1992).
12. S. Strite and H. Morkoc, *J. Vac. Sci. Technol. B*, **10**: 1237(1992).
13. E. Ruiz, S. Alvarez, and Pere Alemany, *Phys. Rev. B*, **49**: 7115 (1994).
14. Fedir Sizov, Zinoviia Tsybrii, Ihor Korotash, and Eduard Rudenko, *IR Blocking and Transparent in Visible and THz Filters* // LAP LAMBERT Academic Publishing; Published on: 2018-08-10. 88 p. ISBN-13: 978-613-9-89803-9.
15. E. Rudenko, Z. Tsybrii, F. Sizov, I. Korotash, D. Polotskiy, M. Skoryk, M. Vuichyk, and K. Svezhentsova, *J. Appl. Phys.*, **121**, No. 13: 135304 (2017).
16. Z. Tsybrii, F. Sizov, M. Vuichyk, I. Korotash, and E. Rudenko, *Infrared Phys.*

Technol., **107**: 103323 (2020).
17. Q. Xia, H. Xia, and A. L. Ruoff, *J. Appl. Phys.*, **73**: 8193 (1993).
18. M. Durandurdu, *J. Alloys and Compd.*, **480**: 917 (2009).
19. L. Hultman, S. Benhenda, G. Radnoczi, J.-E. Sundgren, J. E. Greene, and I. Petrov, *Thin Solid Films*, **215**: 152 (1992).
20. M. Ueno, A. Onodera, O. Shimomura, and K. Takemura, *Phys. Rev. B*, **45**: 10123 (1992).
21. S. Uehara, T. Masamoto, A. Onodera, M. Ueno, O. Shimomura, and K. Takemura, *J. Phys. Chem. Solids*, **58**: 2093 (1997).
22. E. Gabe, Y. LePage, and S. L. Mair, *Phys. Rev. B*, **24**: 5634 (1981).
23. C. Carlone, K. M. Lakin, and H. R. Shanks, *J. Appl. Phys.*, **55**: 4010 (1984).
24. A. T. Collins, E. C. Lightowlers, and P. J. Dean, *Phys. Rev.*, **158**: 833 (1967).
25. V. A. Fomichev, *Fiz. Tverd. Tela (Leningrad)*, **10**, 763 (1968) [*Sov. Phys. Solid. State*, **10**: 597 (1968)].
26. R. V. Kasowski and F. S. Ohuchi, *Phys. Rev. B*, **35**: 9311 (1987).
27. M. Gautier, J. P. Duraud, and C. Le Gressus, *Surf. Sci.*, **178**: 201 (1986).
28. K. Tsubouchi, K. Sugai, and N. Mikoshiba, *In 1981 Ultrasonics Symposia Proceedings, edited by B. R. McAvoy* (IEEE, New York, 1981), p. 375.
29. W. M. Yim, E. J. Stofko, P. J. Zanzucchi, J. I. Pankove, M. Ettenberg, and S. L. Gilbert, *J. Appl. Phys.*, 44: 292 (1973).
30. B. Hejda, *Phys. Status Solidi*, **32**: 407 (1969).
31. S. Bloom, *J. Phys. Chern. Solids*, **32**: 2027 (1971).
32. D. Jones and A. H. Lettington, *Solid State Commun.*, **11**: 701 (1972).
33. W. Y. Ching and B. N. Harmon, *Phys. Rev. B*, **34**: 5305 (1986).
34. A. Kobayashi, O. Sankey, S. M. Yolz, and J. D. Dow, *Phys. Rev. B*, **28**: 935 (1983).
35. L. M. Goldman, R. Twedt, S. Balasubramanian, and S. Sastri, *Proc. SPIE*, 8016 (2011).
36. J. W. McCauley, P. Patel, M. W. Chen, G. Gilde et al, *J. Eur. Ceram. Soc.*, **29**: 223 (2009).
37. H. Li, P. Mina, N. Songa, A. Zhanga et al, *Ceram. Int.*, **45**: 8188 (2019).
38. E. M. Rudenko, V. Ye. Panarin, P. O. Kyrychok, M. Ye. Svavilnyi, I. V. Korotash, O. O. Palyukh, D. Yu. Polotskyi, and R. L. Trishchuk, *Progress in Physics of Metals*, **20**, No. 3: 485 (2019).
39. V. F. Semenyuk, E. M. Rudenko, I. V. Korotash, L. S. Osipov, D. Yu. Polotskiy, K. P. Shamray, V. V. Odinokov, G. Ya. Pavlov, and V. A. Sologub, *Metallofiz. Noveishie Tekhnol.*, **33**, No. 2: 223 (2011).
40. V. F. Semenyuk, V. F. Virko, I. V. Korotash, L. S. Osipov, D. Yu. Polotsky, E. M. Rudenko, V. M. Slobodyan, and K. P. Shamrai, *Probl. At. Sci. Technol.*, **4**: 179 (2013).
41. C. Yeh, Z. W. Lu, S. Froyen, and A. Zunger, *Phys. Rev. B*, **46**: 10086 (1992).
42. D. Singh, *Planewaves, Pseudopotentials and LAPW Method* (Boston: Kluwer Academic: 1994).
43. J. P. Perdew, S. Burke and M. Ernzerhof, *Phys. Rev. Lett.*, **77** (1996).
44. P. Blaha, K. Schwarz, G. K. Madsen et al., *An Augmented Plane Wave + Local Orbitals Program for Calculating Crystal Properties* (Wien: Karlheinz Schwarz Techn. Universiteit: 2001).
45. http://www.wien2k.at/reg_user/faq/
46. J. Murrel, S. Kettle, and J. Tedder, *Teoriya Valentnosti* [Theory of Valence] (Moskva: Mir: 1968).